Distribution of a polymer chain between two interconnected spherical cavities*

Chao Wang(王超)[1,†], Ying-Cai Chen(陈英才)[1], Shuang Zhang(张爽)[2], Hang-Kai Qi(齐航凯)[3], and Meng-Bo Luo(罗孟波)[3,‡]

[1] *Department of Physics, Taizhou University, Taizhou* 318000, *China*
[2] *College of Science, Beibu Gulf University, Qinzhou* 535011, *China*
[3] *Department of Physics, Zhejiang University, Hangzhou* 310027, *China*

(Received 6 July 2020; revised manuscript received 29 July 2020; accepted manuscript online 13 August 2020)

The equilibrium distribution of a polymer chain between two interconnected spherical cavities (a small one with radius R_s and a large one with radius R_l) is studied by using Monte Carlo simulation. A conformational transition from a double-cavity-occupation (DCO) state to a single-cavity-occupation (SCO) state is observed. The dependence of the critical radius of the small cavity (R_{sC}) where the transition occurs on R_l and the polymer length N can be described by $R_{sC} \propto N^{1/3} R_l^{1-1/3\nu}$ with ν being the Flory exponent, and meanwhile the equilibrium number (m_s) of monomers in the small cavity for the DCO phase can be expressed as $m_s = N/((R_l/R_s)^3 + 1)$, which can be quantitatively understood by using the blob picture. Moreover, in the SCO phase, the polymer is found to prefer staying in the large cavity.

Keywords: polymer, phase transition, free energy, blob theory

PACS: 82.35.Jk, 82.35.Lr, 82.20.Wt **DOI:** 10.1088/1674-1056/abaedc

1. Introduction

Study on the statics and dynamics of polymers between two spaces interconnected by a small pore is very important for understanding the exchange of biopolymers in many biological processes, such as transportation of proteins and RNA through channels in biological membranes,[1–3] ejection of DNA from a virus capsid into host cells,[4] *etc*. It is also very helpful for developing related biological nanotechnology, such as genome mapping,[5–9] drug delivery and gene therapy,[10,11] DNA sequencing, controlling, separation and packaging,[12–21] *etc*.

The translocation dynamics of polymer from the *cis* space to the *trans* space through a narrow pore has been studied extensively in the last two decades. To thread through the pore, the polymer has to adopt some special configurations inside the pore since the size of the pore is much smaller than that of the polymer in the free space. That leads to the reduction of the conformation entropy for polymer translocation. Therefore, it is very difficult for the polymer to transfer spontaneously from the *cis* space to the *trans* space. In experiment and simulation, the transferring process can be activated by introducing an external driving force, such as the electrical field force,[19–22] the flow of fluid,[23–25] *etc*. When the driving force is large enough, the polymer can move across the pore and enter into the *trans* space. For a flexible polymer chain slowly dragged by one end into a nanotube from an infinite space, Klushin *et al*. found that the polymer is quickly sucked into the tube and undergoes an obvious phase transition from a flower state to an imprisoned state when the distance of the polymer end from the tube entrance is bigger than a critical value.[26] When the polymer is completely confined in the channel, many configurations are forbidden, but the distribution of polymer is still complicated. Depending on the radius of the channel, there are four scaling regimes,[27] *i.e*., the classic Odijk regime, the transition regime, the extended de gennes regime and the classic de gennes regime, in which different conformation modes are found. Moreover, the conformation of the polymer is also affected by other important factors, such as the flexibility of the polymer,[28–30] the topology of the polymer,[31,32] the geometry of the channel,[33] the flexibility of the channel,[34] *etc*. Klushin *et al*. also predicted that the reverse process, *i.e*., the ejection of polymer from a nanotube into an infinite *trans* space, would occur smoothly without any transition.[26] However, when the *trans* space is finite (*e.g*., a spherical cavity), it was found that there is an obvious phase transition of the polymer from a partially ejected state to a completely ejected state with the increase of the radius of the spherical cavity.[35] For a flexible polymer initially confined in a small spherical cavity connected by an infinite *trans* space, the polymer can escape eventually from the cavity because of so-called entropic force.[36,37] However, when the attractive interaction between the polymer and the inner wall of the cavity is considered,

*Project supported by the Natural Science Foundation of Zhejiang Province, China (Grant No. LY20A040004) and the National Natural Science Foundation of China (Grant Nos. 11604232, 11674277, 11704210, and 11974305).

†Corresponding author. E-mail: chaowang0606@126.com
‡Corresponding author. E-mail: luomengbo@zju.edu.cn

phase transition from an ejected state to a packaged state is found.[38] When the polymer is completely confined in a single cavity, the polymer may be desorbed or adsorbed, depending on the strength of the attraction between polymer and the wall of the cavity.[39] Moreover, there are more conformation transitions in a single cavity, such as coil–helix transition of semiflexible polymers,[40] entropy-induced separation of binary semiflexible ring polymer mixtures,[41] and DNA compaction transition,[42] *etc*.

Recently, Cifra *et al.* have studied the conformation and distribution of flexible and semiflexible polymers in an array of nanoposts, and found that the polymer can be confined in one of the channel-like interstitial volumes between nanoposts or partition among these volumes, depending on the chain stiffness and the crowding effect imposed by nanoposts.[43–46] This is similar to the distribution behavior of polymer confined in two interconnected cavities.[47–50] Experimentally, Nykypanchuk *et al.* have studied the partitioning of a single DNA in two interconnected spherical cavities prepared by the colloidal templating method.[48] For the weakly or moderately confined case, the DNA chain is found to maximize its configurational entropy by partitioning toward the larger cavity. While for the strongly confined case, the DNA chain is observed to occupy both the two cavities and split its segments between the two cavities.[48] Simulationly, Cifra *et al.* have studied the partitioning of flexible or semiflexible polymers between two interconnected spherical cavities.[49,50] Based on the distribution probability of segment in one of the cavity, the free energy landscape was calculated. With the increase of the polymer length or the decrease of the size of the cavities, it was found that the convex curvature in middle region of the free energy landscape turns gradually into a concave curvature, indicating that the polymer undergoes a conformational transition from the single cavity occupation to the conformation bridging the two cavities.[49] However, it is difficult to obtain the critical parameter conditions of the transition from the free energy landscape, and then the phase diagram and the corresponding physical mechanisms are not clear yet.

In this work, the equilibrium distribution of a polymer chain between two interconnected spherical cavities (a small one with radius R_s and a large one with radius R_l) is studied by using Monte Carlo simulation. Depending on the size of the cavities, we find an obvious phase transition between a single-cavity-occupation state, where all the monomers of the polymer are in one of the cavities, and a double-cavity-occupation state, where the polymer adopts conformations bridging the two cavities. The main objective of the present work is to obtain the relations between the polymer length and the the critical size of the cavities where the transition occurs, and uncover the corresponding physical mechanisms by using the blob theory.

2. Simulation model and method

Simulations are carried out in three-dimensional (3D) space. Figure 1 shows a two-dimensional (2D) sketch of the simulation geometry and the polymer model used in simulation. Two spherical cavities (the small one and the large one) are connected by a small hole. The radii of the small and the large cavities are R_s and R_l, respectively, and the diameter of the hole is D_h. The polymer is confined in the two cavities.

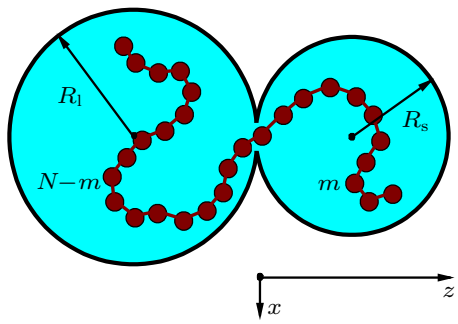

Fig. 1. A 2D sketch of the simulation model. Two spherical cavities, a small one with radius R_s and a large one with radius R_l, are connected by a small hole with diameter D_h. The polymer is confined in the two cavities.

The polymer is modeled as a coarse-grained off-lattice bead spring chain.[51] In this model, the polymer with length N is formed by N identical monomers connected sequentially by bonds. There are only two types of interactions: bonded interaction between bonded monomers and non-bonded interaction between non-bonded monomers. The bonded interaction is described by the finitely extensible nonlinear elastic (FENE) potential

$$U_{\mathrm{FENE}} = -\frac{k_{\mathrm{F}}}{2}(b_{\max}-b_0)^2 \ln\left[1-\left(\frac{b-b_0}{b_{\max}-b_0}\right)^2\right] \tag{1}$$

with the spring constant $k_{\mathrm{F}} = 40$, the average bond length $b_0 = 0.7$, the maximum bond length $b_{\max} = 1$, and the minimum bond length $b_{\min} = 0.4$.[51] Here b is the bond length. The non-bonded interaction is described by the Morse potential

$$U_{\mathrm{M}}(r) = \begin{cases} \varepsilon\{\exp[-2\alpha_{\mathrm{M}}(r-r_{\min})]-2\exp[-\alpha_{\mathrm{M}}(r-r_{\min})]\}-U_{\mathrm{cut}}, & r \le r_{\mathrm{cut}}, \\ 0, & r > r_{\mathrm{cut}}, \end{cases} \tag{2}$$

where $\alpha_{\mathrm{M}} = 24$, $r_{\min} = 0.8$, $r_{\mathrm{cut}} = 1$, $\varepsilon = 1$,[51] and U_{cut} is a special value that ensures $U_{\mathrm{M}}(r_{\mathrm{cut}}) = 0$. There is only steric interaction between the monomer and the inner wall of the two cavities.

Monte Carlo method is adopted to mimic the motion of the monomer. For each trial move, we randomly selected a monomer and change its position with a random displacement $\Delta \boldsymbol{r} = \Delta x\boldsymbol{i} + \Delta y\boldsymbol{j} + \Delta z\boldsymbol{k}$, where Δx, Δy, and Δz are chosen randomly from the interval $(-0.25,\ 0.25)$. Based on the the standard Metropolis algorithm, the new position of the selected monomer is accepted with a probability $\min[1, \exp(-\Delta U/k_{\rm B}T)]$, where ΔU represents the energy change caused by the trial move. The time unit is one Monte Carlo step (MCS) during which N moves are tried.

The whole polymer is in the large cavity at the beginning of the simulation. We at first run a sufficiently long time t_0 to equilibrate the polymer, and then counter the number of monomers ($m_{\rm s}$) in the small sphere. Here, $m_{\rm s} = 0$ or N indicates that the whole polymer occupies only one of the two cavities, *i.e.*, the polymer is at the single-cavity-occupation state (the SCO state). Specifically, the whole polymer is in the large cavity for $m_{\rm s} = 0$ and in the small cavity for $m_{\rm s} = N$. While $0 < m_{\rm s} < N$ implies that the whole polymer occupies the two cavities simultaneously, *i.e.*, the polymer is at the double-cavity-occupation state (the DCO state). The result of $m_{\rm s}$ shown in this work are averaged over $n_{\rm sam}$ $(= 10^4)$ independent samples. The probabilities of the whole polymer in the small cavity ($P_{\rm s}$) and in the large cavity ($P_{\rm l}$) are defined as $n_{\rm s}/n_{\rm sam}$ and $n_{\rm l}/n_{\rm sam}$, respectively, where $n_{\rm s}$ and $n_{\rm l}$ are the number of samples satisfying $m_{\rm s} = N$ and $m_{\rm s} = 0$, respectively. Therefore, the probability of the SCO state $P_{\rm SCO} = P_{\rm s} + P_{\rm l}$.

In this work, $k_{\rm B}T$ and $b_{\rm max}$ are set as the units of energy and length, respectively, where $k_{\rm B}$ is the Boltzmann constant and T is the temperature. In our model, the size of the hole is an important parameter. It determines the equilibrium time for the polymer reaching the finial equilibrium state, but dose not influence the equilibrium distribution of the polymer between the two cavities. When the hole size is big, the polymer can reach the finial equilibrium state quickly, but the fluctuation of the equilibrium distribution is large. Therefore, we here chose a relatively small hole with diameter $D_{\rm h} = 0.2$ to ensure the monomers pass through the hole one by one. Correspondingly, we chose a large enough t_0 $(> 10^7)$ to equilibrate the polymer.

3. Results and discussion

3.1. The symmetric twin-cavity system

At first, the equilibrium distribution of polymer in the symmetric twin-cavity system ($R_{\rm s} = R_{\rm l} = R$) is studied. Figure 2 shows the dependence of the SCO probability $P_{\rm SCO}$ on the radius of the cavity R for different $N_{\rm s}$. We can see that $P_{\rm SCO}$ as a function of R contains three different regimes. In the small R regime, $P_{\rm SCO}$ is nearly 0, meaning that the polymer adopts configurations bridging the two cavities, *i.e.*, the polymer is at the DCO state. In the large R regime, $P_{\rm SCO}$ is roughly 1, indicating that the whole polymer is in one of the two cavities, *i.e.*, the polymer is at the SCO state. In the moderate R regime, $P_{\rm SCO}$ increases quickly from 0 to 1 with increasing R, *i.e.*, a phase transition from the DCO state to the SCO state occurs. To give approximately the position of the phase transition, we here define the radius of the cavity where $P_{\rm SCO} = 0.5$ as the critical radius $R_{\rm C}$, as shown in Fig. 2. $R_{\rm C}$ is dependent on the polymer length N. With N increasing, the size of each cavity that can accommodate the whole polymer is bigger and bigger, leading to the monotonous increase of $R_{\rm C}$ with N. We find that the dependence of $R_{\rm C}$ on N can be specifically described by a simple scaling relation $R_{\rm C} \propto N^{0.59}$, as shown in the inset of Fig. 2. Interestingly, for any given N, the critical radius $R_{\rm C}$ is roughly equal to the radius of gyration ($R_{\rm g0}$) of polymer in free space, as shown the red line in the inset of Fig. 2.

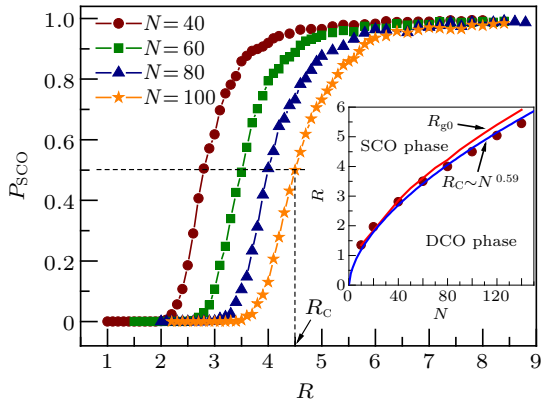

Fig. 2. The SCO probability $P_{\rm SCO}$ as a function of R for different N. The radius where $P_{\rm SCO} = 0.5$ is defined as the critical radius $R_{\rm C}$. The inset shows the phase diagram for the symmetric twin-cavity system. The red line shows the radius of gyration ($R_{\rm g0}$) of polymer in free space as a function of N.

3.2. The asymmetric system

We then studied the equilibrium distribution of polymer in the asymmetric system ($R_{\rm s} < R_{\rm l}$). Figure 3 shows the dependence of the SCO probability $P_{\rm SCO}$ on the radius of the small cavity $R_{\rm s}$ for different radii of large cavity $R_{\rm l}$ ($< R_{\rm C}$, $R_{\rm C}$ is the critical radius of the cavity for the symmetric twin-cavity system), where $N = 60$ and the corresponding $R_{\rm C} = 3.5$ (as shown in the inset of Fig. 2). We can see that there is also an obvious transition from $P_{\rm SCO} = 1$ (the SCO state) to $P_{\rm SCO} = 0$ (the DCO state) with increasing $R_{\rm s}$. Similarly, we define the radius of the small cavity where $P_{\rm SCO} = 0.5$ as the critical radius $R_{\rm sC}$, as shown in Fig. 3. $R_{\rm sC}$ is dependent on the size of the large cavity and the length of the polymer. With $R_{\rm l}$ decreasing or N increasing, the confinement effect of the cavities on the polymer is stronger and stronger, which would compel the polymer to adopt bridging configurations between the two cavities to maximize the conformational entropy at relatively small value of $R_{\rm s}$, leading to the monotonous decrease of $R_{\rm sC}$ with decreasing $R_{\rm l}$ or increasing N. We find that the

monotonous dependence of R_{sC} on R_l and N can be specifically expressed as $R_{sC} \sim R_l^{9/4}N^{-3/4}$, as shown in the inset of Fig. 4. Based on R_{sC}, we can also specifically define the two equilibrium states (phases) when $R_l < R_C$: the DCO phase at $R_s > R_{sC}$ and the SCO phase at $R_s < R_{sC}$, as shown in Fig. 4. However, when R_l is large ($R_l > R_C$), we find that P_{SCO} is always bigger than 0.5 for any given R_s (results not shown), *i.e.*, there is only the SCO state when $R_l > R_C$, as shown in Fig. 4.

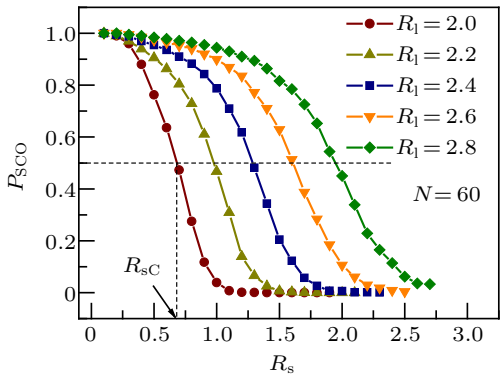

Fig. 3. The SCO probability P_{SCO} as a function of the radius of the small cavity R_s for different R_l ($< R_C$), where $N = 60$. The radius where $P_{SCO} = 0.5$ is defined as the critical radius R_{sC}.

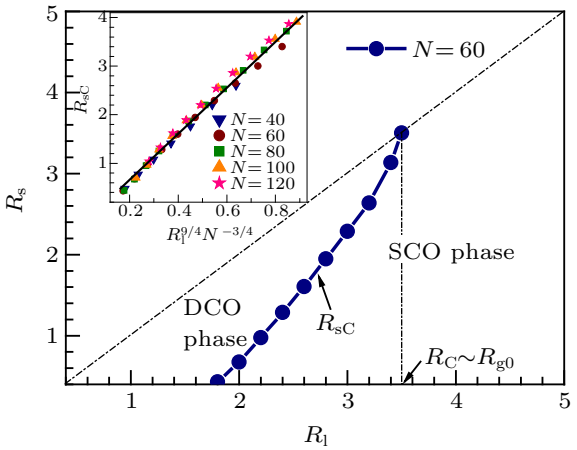

Fig. 4. Phase diagram for the asymmetric system, where $N = 60$. The inset shows the dependence of R_{sC} on $R_l^{9/4}N^{-3/4}$ for $N = 40$, 60, 80, 100, and 120. The solid black line is guide for eyes.

In the SCO phase, the whole polymer is in one of the two cavities. But it is not necessary that the whole polymer is in the small cavity and in the large cavity with the same probability. Figure 5 shows the dependence of the relative probabilities of the whole polymer in the small cavity (P_s/P_{SCO}) and in the large cavity (P_l/P_{SCO}) on the radius of the small cavity R_s for different R_l, where $N = 60$. We can see that P_l is always larger than P_s for any given R_s and R_l ($R_s < R_l$), meaning that the polymer prefers occupying the large cavity to maximize the conformational entropy in the SCO phase. However, at $R_s = R_l$ (the symmetric twin-cavity case), P_s is nearly equal to P_l, and then $P_s/P_{SCO} = P_l/P_{SCO} = 0.5$, *i.e.*, the whole polymer in the small cavity and in the large cavity with the same probability.

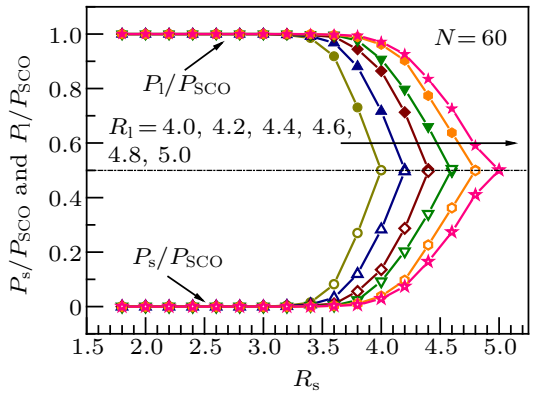

Fig. 5. The relative probabilities of the whole polymer in the small cavity (P_s/P_{SCO}) and in the large cavity (P_l/P_{SCO}) in the SCO phase as functions of the radius of the small cavity R_s for different R_l, where $N = 60$.

In the DCO phase, both the two cavities are occupied by the polymer. Figure 6 shows the dependence of the equilibrium number (m_s) of monomers in the small cavity on R_s for different R_l ($< R_C$), where $N = 60$. Based on the critical radius R_{sC}, two different regions are found. When $R_s < R_{sC}$, m_s is nearly to be zero, *i.e.*, the whole polymer is in the large cavity. While when $R_s > R_{sC}$, m_s increases monotonously with increasing R_s and reaches $N/2$ at $R_s = R_l$, *i.e.*, the polymer splits its segments between the two cavities. For any given R_s ($> R_{sC}$), m_s increases monotonously with decreasing R_l, because the confinement effect of the large sphere on the polymer is stronger and stronger with decreasing R_l, as shown in Fig. 6.

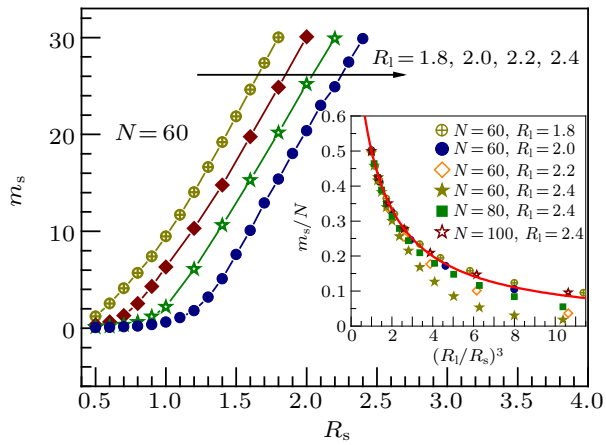

Fig. 6. The equilibrium number (m_s) of monomers in the small cavity as a function of R_s for different R_l ($< R_C$), where $N = 60$. The inset shows m_s/N as a function of $(R_l/R_s)^3$ for different R_l and N. The solid red line is given by Eq. (12).

In their experiment work, Nykypanchuk *et al* have study the partitioning of fluorescently labeled a single DNA chain with different length within two interconnected spherical cavities with different size.[48] For the case R_{g0} is bigger than the radius (R) of the equal-sized cavities (strong confinement case), the DNA chain prefers to adopt bridging configuration with equal subchain length in the two cavities, *i.e.*, the DNA chain is in the DCO phase, which is in good agreement with the simulation results shown in the inset of Fig. 2 and Fig. 6.

While for the case R_{g0} is much less than R_l or R_s (weak and moderate confinement case), it was found that the probability for DNA bridging the two cavities is very small, and the whole DNA is confined in one of the two cavities, *i.e.* the DNA chain is in the SCO phase, which is in good agreement with the phase diagram shown in Fig. 4. Moreover, it was found that the time for DNA spent in the large cavity is longer than that in the small cavity, *i.e.*, the probability of the whole DNA in the large cavity is bigger than that in the small cavity, which is also in agreement with the simulation results shown in Fig. 5.

The scaling relation of R_C on N and that of R_{sC} on R_l and N can be understood by using the blob picture. For a polymer chain confined in a small spherical cavity, the polymer can be envisioned as a compact stacking of blobs of size ξ in the sphere. In each blob, the confinement effect of the cavity can be neglected, and the internal correlations between monomers are the same as those in the bulk. The blob size ξ is dependent on the polymer length N and the diameter of the spherical cavity D, *i.e.*, ξ decreases with increasing N or decreasing D, which can be specifically expressed as[52]

$$\xi \sim \left(\frac{D^3}{N}\right)^{\nu/(3\nu-1)} \tag{3}$$

with ν $(=3/5)$ the Flory exponent for a three-dimensional self-avoiding polymer chain. The number of blobs (n_b) in the cavity can then be written as $n_b \sim D^3/\xi^3$.[52] Based on the blob theory, the blob is the basic element of the free energy of the polymer, and the free energy F (in unit of k_BT) is proportional to the number of blobs, *i.e.*,[52]

$$F \sim \frac{D^3}{\xi^3}. \tag{4}$$

Assuming there are m monomers in the small cavity and N–m monomers in the large cavity, the polymer can be viewed as two tethered chains, and the free energy (F) of the polymer can then be written as

$$F \sim \frac{R_s^3}{\xi_s^3} + \frac{R_l^3}{\xi_l^3}. \tag{5}$$

Here, $\xi_s \sim R_s^{3\nu/(3\nu-1)} m^{\nu/(1-3\nu)}$ and $\xi_l \sim R_l^{3\nu/(3\nu-1)}(N-m)^{\nu/(1-3\nu)}$ represent the blob size in the small cavity and the large cavity, respectively. For given R_s, R_l, and N, the relation between ξ_s and ξ_l at the thermal equilibrium state is determined by

$$\mathrm{d}F/\mathrm{d}\xi_s = 0. \tag{6}$$

This leads to

$$\frac{R_s^3}{\xi_s^4} + \frac{R_l^3}{\xi_l^4}\frac{\mathrm{d}\xi_l}{\mathrm{d}\xi_s} = 0. \tag{7}$$

From the expressions of ξ_s and ξ_l, we can also obtain $N \sim R_s^3/\xi_s^{3-1/\nu} + R_l^3/\xi_l^{3-1/\nu}$, *i.e.*,

$$\xi_l = R_l^{3\nu/(3\nu-1)}\left(N - \frac{R_s^3}{\xi_s^{3-1/\nu}}\right)^{\nu/(1-3\nu)}. \tag{8}$$

We then get

$$\frac{\mathrm{d}\xi_l}{\mathrm{d}\xi_s} = -\frac{R_s^3}{R_l^3}\frac{\xi_l^{4-1/\nu}}{\xi_s^{4-1/\nu}}. \tag{9}$$

Substituting Eq. (9) into Eq. (7), we can then obtain

$$\xi_s = \xi_l, \tag{10}$$

i.e., the size of the blob in the small cavity is the same as that in the large cavity at the thermal equilibrium state, which can be used as a criterion to judge whether the polymer is at the equilibrium state or not.

Based on this criterion, we can then define a critical radius of the small cavity R_{sC}, where the size of the small cavity is just equal to the blob size when the whole polymer is in the large cavity, *i.e.*,

$$R_{sC} \sim \left(\frac{R_l^3}{N}\right)^{\nu/(3\nu-1)}. \tag{11}$$

Obviously, $\xi_s = \xi_l$ can only occur when $R_s > R_{sC}$, *i.e.*, the polymer is in the DCO phase when $R_s > R_{sC}$. When $R_s < R_{sC}$, it is difficult for polymer to enter into the small cavity, *i.e.*, the whole polymer is in the large cavity and the polymer is in the SCO phase. Substituting the Flory exponent $\nu = 3/5$ into Eq. (11), we can then get $R_{sC} \sim R_l^{9/4}N^{-3/4}$, which are in good agreement with the simulation results, as shown in the inset of Fig. 4. Moreover, substituting $\xi_s \sim R_s^{3\nu/(3\nu-1)}m^{\nu/(1-3\nu)}$ and $\xi_l \sim R_l^{3\nu/(3\nu-1)}(N-m)^{\nu/(1-3\nu)}$ into Eq. (10), we can obtain the dependence of the equilibrium number of monomers (m_s) in the small cavity in the DCO phase on R_s, R_l, and N, *i.e.*,

$$m_s = \frac{N}{(R_l^3/R_s^3+1)}, \tag{12}$$

which is also in good agreement with the simulation results when $m_s \gg 0$, as shown with the solid red line in the inset of Fig. 5. When $m_s \to 0$, the polymer is out of the DCO phase, so the dependence of m_s on R_s, R_l, and N deviates from Eq. (12) gradually, as shown in the inset of Fig. 5.

For the symmetric twin-cavity system ($R_s = R_l = R$), we can obtain the relation between the critical radius R_C and the polymer length N from Eq. (11), *i.e.*, $R_C \sim N^\nu$, which is in good agreement with the simulation result, as shown in the inset of Fig. 2. Meanwhile, we can get $m_s = N/2$ or $m_s/N = 0.5$ from Eq. (12), *i.e.*, each of the two cavities accommodates half number of monomers, which is also in good agreement with the simulation result, as shown in Fig. 6.

4. Conclusion

In this work, the equilibrium distribution of a polymer chain between two interconnected spherical cavities (a small one with radius R_s and a large one with radius R_l) is studied by using Monte Carlo simulation. A continuous phase transition from a double-cavity-occupation (DCO) state to a single-cavity-occupation (SCO) state is observed with increasing the size of the two cavities. For the symmetric twin-cavity system ($R_s = R_l = R$), the dependence of the critical cavity radius (R_C) where the transition occurs on the polymer length (N) can be expressed as $R_C \propto N^{\nu}$ with the ν being the Flory exponent. For the asymmetric system, the dependence of the critical radius of the small cavity (R_{sC}) on R_l and N can be described by $R_{sC} \propto N^{1/3} R_l^{1-1/3\nu}$, and meanwhile the equilibrium number (m_s) of monomers in the small cavity for the DCO phase can be expressed as $m_s = N/((R_l/R_s)^3 + 1)$. By theoretical analysis based on the blob picture, it is found that the phase transitions are determined by the blob size of polymer in the small sphere and the large sphere, respectively. Our results maybe helpful for understanding the injection of DNA into a bacteria cell from a virus capsid.

References

[1] Simon S M and Blobe G 1991 *Cell* **65** 371
[2] Lingappa V R, Chaidez J, Yost C S and Hedgpeth J 1984 *Proc. Natl. Acad. Sci. USA* **81** 456
[3] Gabashvili I S, Gregory S T, Valle M, Grassucci R, Worbs M, Wahl M C, Dahlberg A E and Frank J 2001 *Mol. Cell* **8** 181
[4] Laemmli U K and Favre M 1973 *J. Mol. Biol.* **80** 575
[5] Levy S L and Craighead H G 2010 *Chem. Soc. Rev.* **39** 1133
[6] Reisner W, Pedersen J N and Austin R H 2012 *Rep. Prog. Phys.* **75** 106601
[7] Lacroix J, Pelofy S, Blatche C, Pillaire M J, Huet S, Chapuis C, Hoffmann J S and Bancaud A 2016 *Small* **12** 5963
[8] Dorfman K D, King S B, Olson D W, Thomas J D P and Tree D R 2013 *Chem. Rev.* **113** 2584
[9] Sriram K K, Yeh J W, Lin Y L, Chang Y R and Chou C F 2014 *Nucleic Acids Res.* **42** e85
[10] Glasgow J and Tullman-Ercek D 2014 *Appl. Microbiol. Biotechnol.* **98** 5847
[11] Chen J X, Chen Y G and Kapral R 2018 *Adv. Sci.* **5** 1800028
[12] Cui R F, Chen Q H and Chen J X 2020 *Nanoscale* **12** 12275
[13] Kasianowicz J J, Brandin E, Branton D and Deamer D W 1996 *Proc. Natl. Acad. Sci. USA* **93** 13770
[14] Deamer D, Akeson M and Branton D 2016 *Nat. Biotechnol.* **34** 518
[15] Yuan Z S, Liu Y M, Dai M, Yi X and Wang C Y 2020 *Nanoscale Res. Lett.* **15** 80
[16] Steinbock L J and Radenovic A 2015 *Nanotechnology* **26** 074003
[17] Tyson J R, O0Neil N J, Jain M, Olsen H E, Hieter P and Snutch T P 2018 *Genome Res.* **28** 266
[18] He Y, Tsutsui M, Fan C, Taniguchi M and Kawai T 2011 *ACS Nano* **5** 5509
[19] Liu X, Zhang Y, Nagel R, Reisner W and Dunbar W B 2019 *Small* **15** 1901704
[20] Mulero R, Prabhu A S, Freedman K J and Kim M J 2010 *J. Assoc. Lab. Autom.* **15** 243
[21] Smith D E, Tans S J, Smith S B, Grimes S, Anderson D L and Bustamante C 2001 *Nature* **413** 748
[22] Meller A, Nivon L and Branton D 2001 *Phys. Rev. Lett.* **86** 3435
[23] Sakaue T, Raphaël E, de Gennes P G and Brochard-Wyart F 2005 *Europhys. Lett.* **72** 83
[24] Markesteijn A P, Usta O B, Ali I, Balazs A C and Yeomans J M 2009 *Soft Matter* **5** 4575
[25] Li X, Pivkin I V and Liang H 2013 *Polymer* **54** 4309
[26] Klushin L I, Skvortsov A M, Hsu H P and Binder K 2008 *Macromolecules* **41** 5890
[27] Reisner W, Pedersen J N and Austin R H 2012 *Rep. Prog. Phys.* **75** 106601
[28] Cifra P, Benkova Z and Bleha T 2009 *J. Phys. Chem. B* **113** 1843
[29] Cifra P 2009 *J. Chem. Phys.* **131** 224903
[30] Fu Y, Wu F, Huang J H, Chen Y C and Luo M B 2019 *Chin. J. Polym. Sci.* **37** 1290
[31] Benkova Z and Cifra P 2012 *Macromolecules* **45** 2597
[32] Benkova Z and Cifra P 2013 *Biochem. Soc. T.* **41** 625
[33] Manneschi C, Angeli E, Ala-Nissila T, Repetto L, Firpo G and Valbusa U 2013 *Macromolecules* **46** 4198
[34] Chen J Z Y 2007 *Phys. Rev. Lett.* **98** 088302
[35] Wang C, Wu F, Zhao B, Chen Y C and Luo M B 2020 *Macromolecules* **53** 1694
[36] Muthukumar M 2001 *Phys. Rev. Lett.* **86** 3188
[37] Turner S W P, Cabodi M and Craighead H G 2002 *Phys. Rev. Lett.* **88** 128103
[38] Matsuyama A, Yano M and Matsuda A 2009 *J. Chem. Phys.* **131** 105104
[39] Shojaei H R and Muthukumar M 2017 *J. Chem. Phys.* **146** 244901
[40] Yang Z Y, Zhang D, Zhang L X, Chen H P, Ateeq-ur-Rehman and Liang H J 2011 *Soft Matter* **7** 6836
[41] Zhou X L, Guo F C, Li K, He L L and Zhang L X 2019 *Polymers* **11** 1992
[42] Chen E, Fan Y, Zhao G, Mao Z, Zhou H and Liu Y 2020 *Chin. Phys. B* **29** 018701
[43] Benkova Z, Rispanova L and Cifra P 2020 *Polymers* **12** 1064
[44] Rispanova L, Benkova Z and Cifra P 2018 *Polymers* **10** 1301
[45] Benkova Z, Rispanova L and Cifra P 2017 *J. Chem. Phys.* **147** 134907
[46] Benkova Z, Rispanova L and Cifra P 2017 *Polymers* **9** 313
[47] Kong C Y and Muthukumar M 2004 *J. Chem. Phys.* **120** 3460
[48] Nykypanchuk D, Strey H H and Hoagland D A 2005 *Macromolecules* **38** 145
[49] Cifra P 2005 *Macromolecules* **38** 3984
[50] Cifra P, Linse P and Nies E 2005 *J. Phys. Chem. B* **112** 8923
[51] Milchev A, Klushin L, Skvortsov A and Binder K 2010 *Macromolecules* **43** 6877
[52] Sakaue T and Raphaël E 2006 *Macromolecules* **39** 2621